Enhancing multiphoton absorption in atomically precise $(AuAg)_{13}$ clusters via 2-/4-mercaptopyridine ligand positional isomerism

Anqi Xu,[‡,a] Ye Wang ,[‡,a] Daqiao Hu,[a] Shengli Li,[*,a] Lin Xiong, [*,b] Shan Jin, [*, c] Qiong Zhang,[a] Manzhou Zhu[a,c]

a. School of Chemistry and Chemical Engineering, Anhui University, Hefei 230601, China.

b. School of Food and Chemical Engineering, Shaoyang University, Shaoyang 422000, P. R. China.

c. Institutes of Physical Science and Information Technology, Key Laboratory of Structure and Functional Regulation of Hybrid Materials of Ministry of Education, Anhui University, Hefei 230601, China.

‡ Anqi Xu and Ye Wang contributed equally to this work.

E-mail: jinshan@ahu.edu.cn; 96044@ahu.edu.cn; linxiong@hnsyu.edu.cn

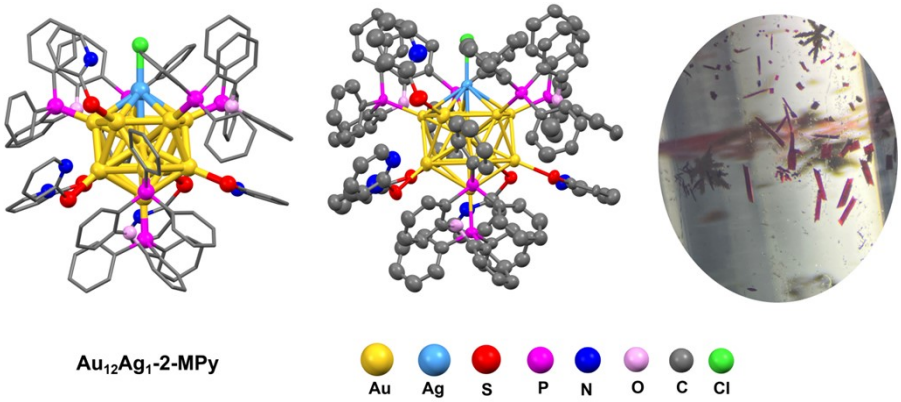

Figure S1. The overall structure of **$Au_{12}Ag_1$-2-MPy** and the corresponding crystal photographs.

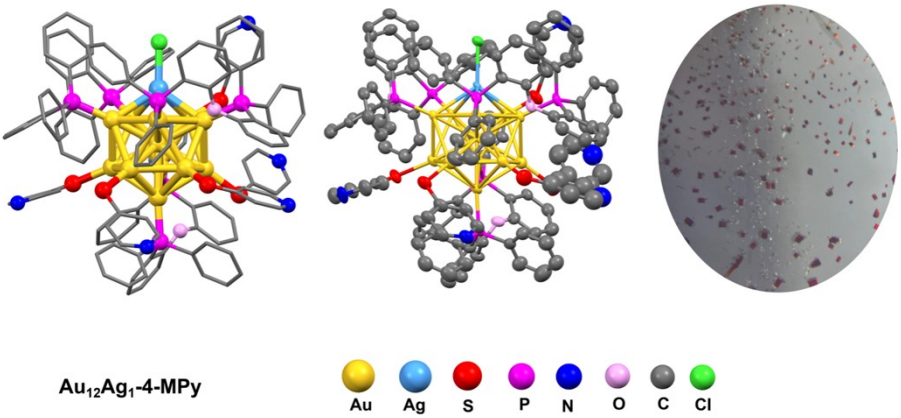

Figure S2. The overall structure of **$Au_{12}Ag_1$-4-MPy** and the corresponding crystal photographs.

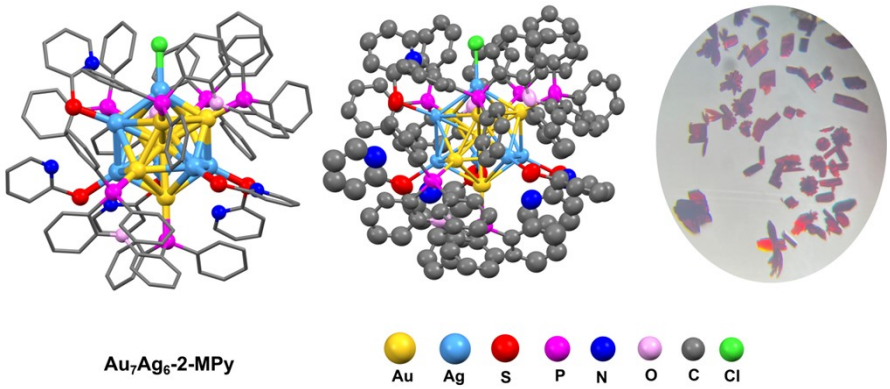

Figure S3. The overall structure of **Au_7Ag_6-2-MPy** and the corresponding crystal photographs.

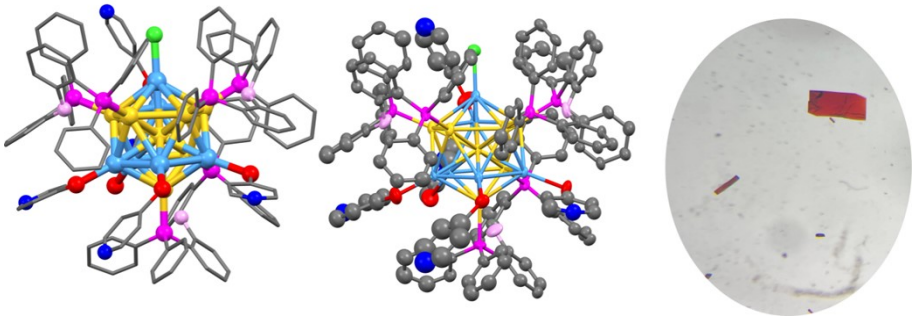

Figure S4. The overall structure of **Au_7Ag_6-4-MPy** and the corresponding crystal photographs.

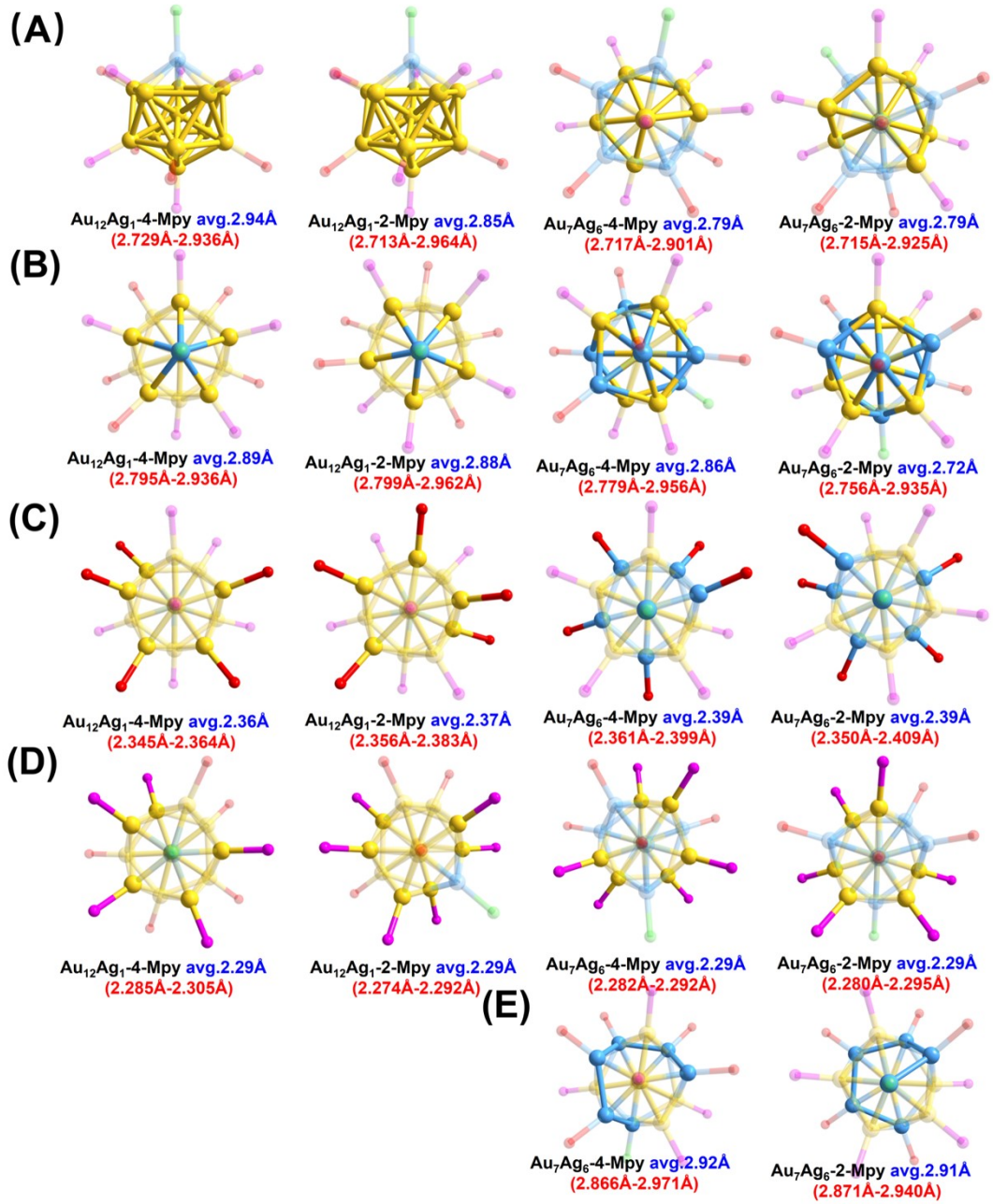

Figure S5. Comparison of the lengths of (A) Au-Au, (B) Au-Ag, (C) M(Au/Ag)-S, (D) Au-P, (E) Ag-Ag bonds of **$Au_{12}Ag_1$-4-MPy**, **$Au_{12}Ag_1$-2-MPy**, **Au_7Ag_6-4-MPy** and **Au_7Ag_6-2-MPy** nanoclusters. Color labels: light orange = Au; blue=Ag; pink = P; red = S. All H atoms were omitted for clarity.

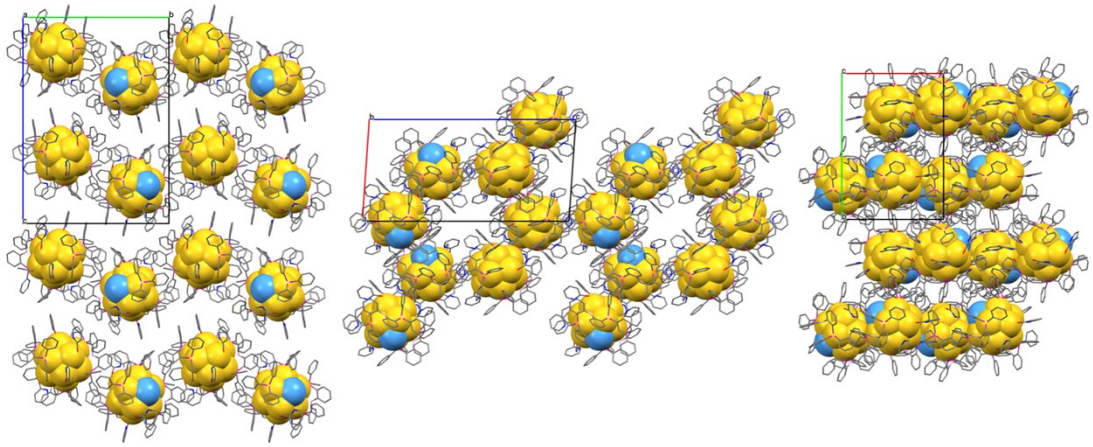

Figure S6. The packing of **$Au_{12}Ag_1$-2-MPy**.

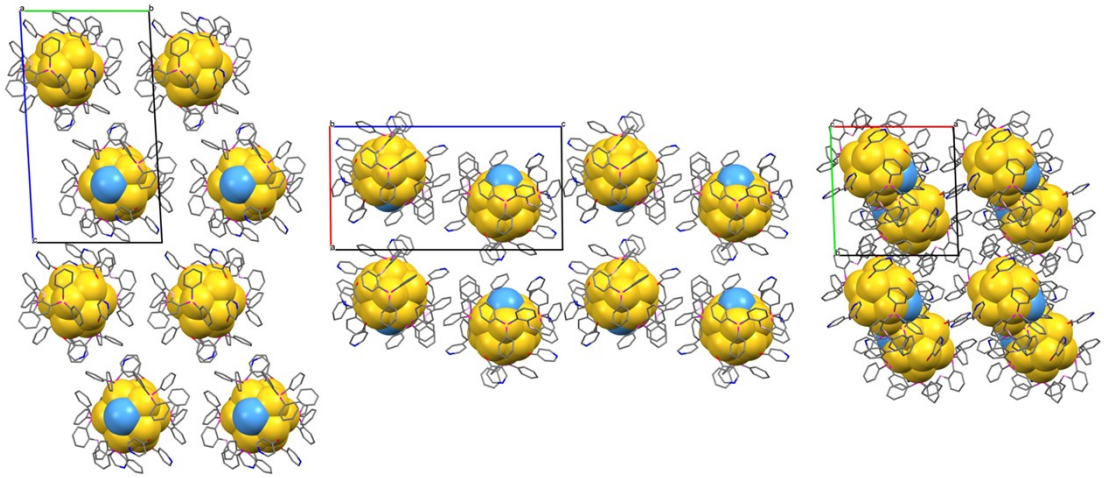

Figure S7. The packing of **$Au_{12}Ag_1$-4-MPy**.

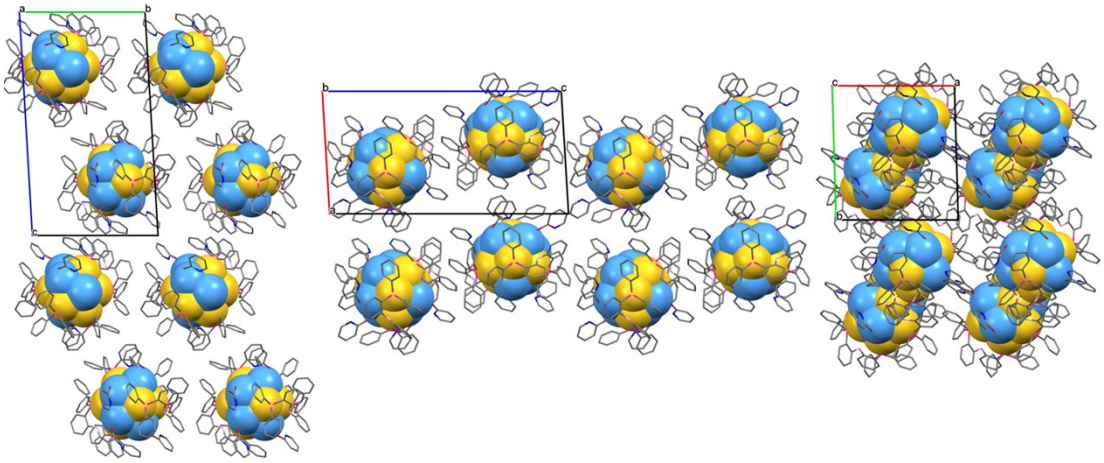

Figure S8. The packing of **Au_7Ag_6-2-MPy**.

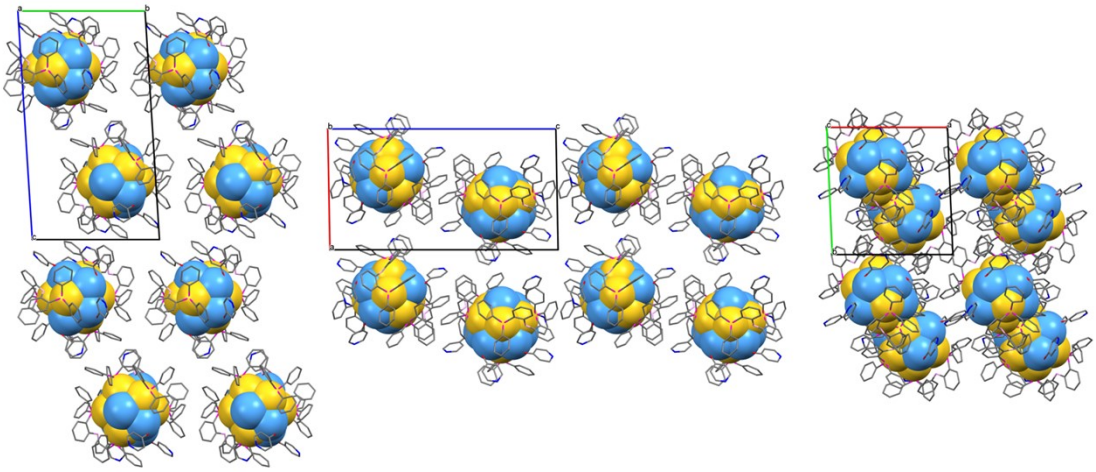

Figure S9. The packing of **Au_7Ag_6-4-MPy**.

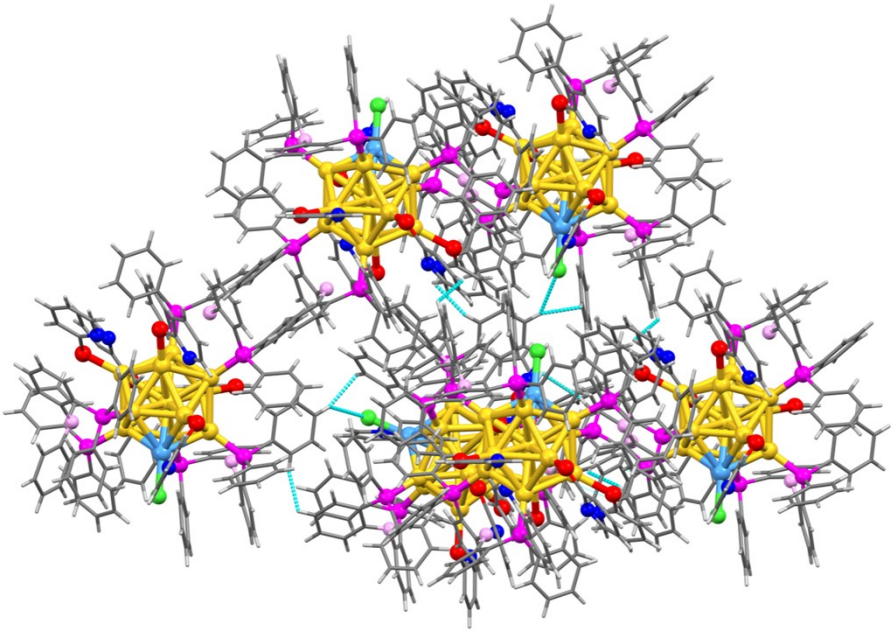

Figure S10. The intermolecular interactions in **$Au_{12}Ag_1$-2-MPy**.

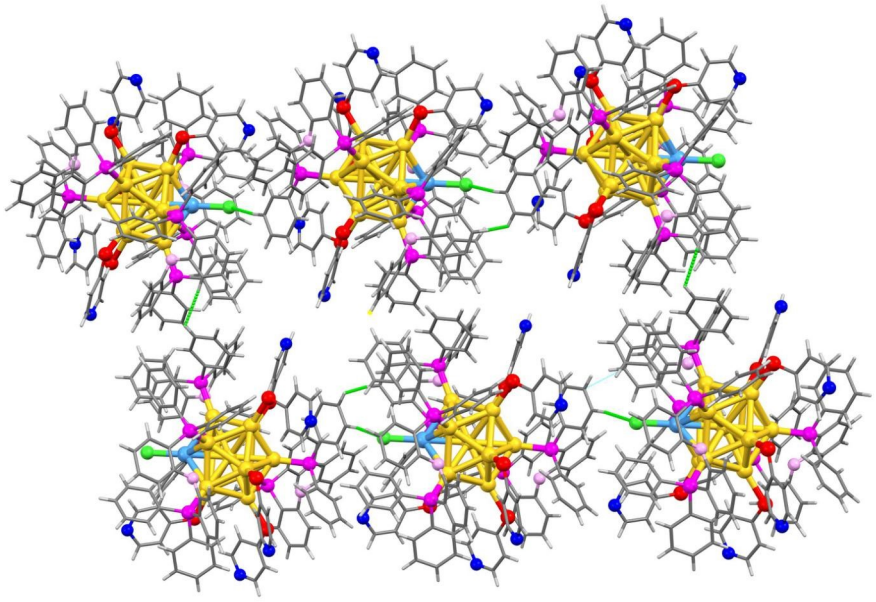

Figure S11. The intermolecular interactions in **$Au_{12}Ag_1$-4-MPy**.

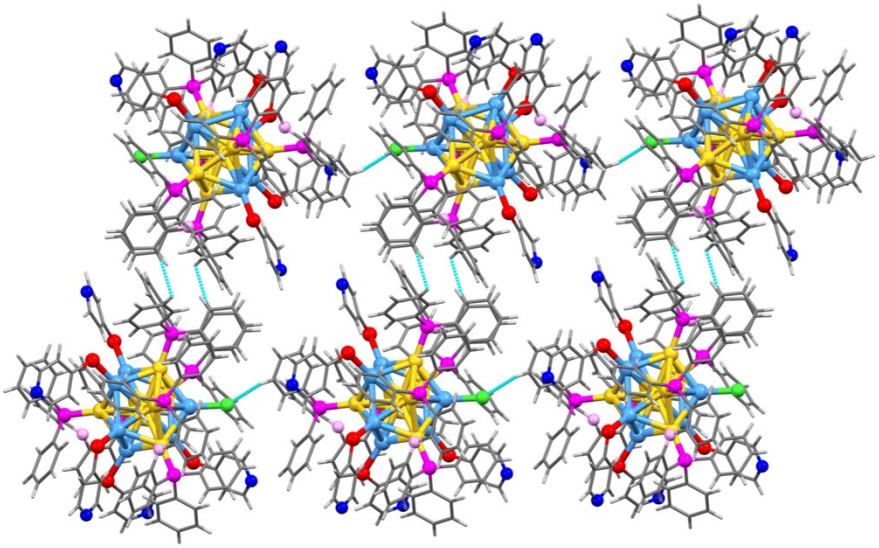

Figure S12. The intermolecular interactions in **Au_7Ag_6-4-MPy**.

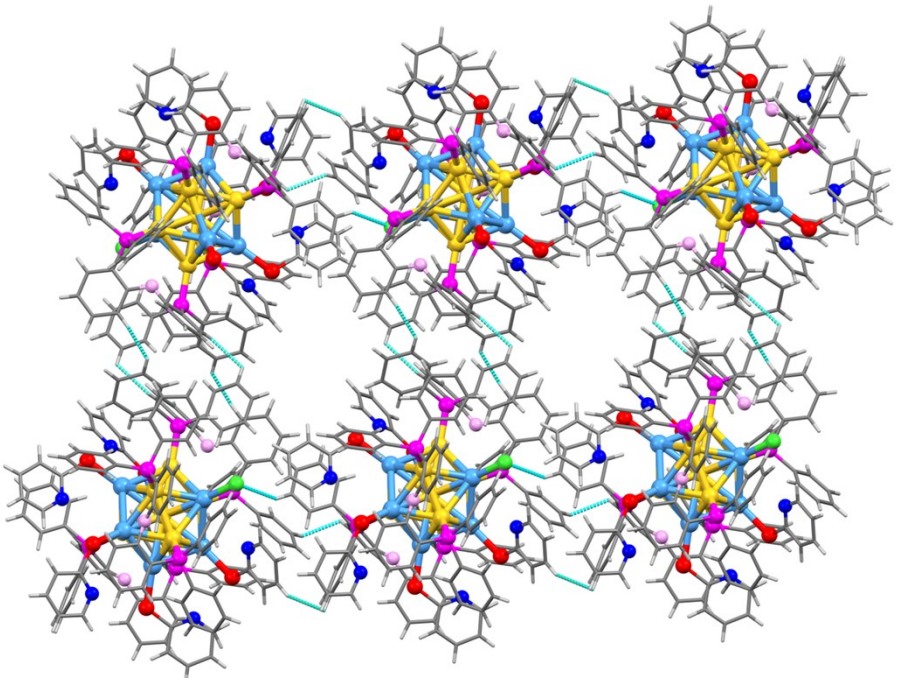

Figure S13. The intermolecular interactions in **Au_7Ag_6-2-MPy**.

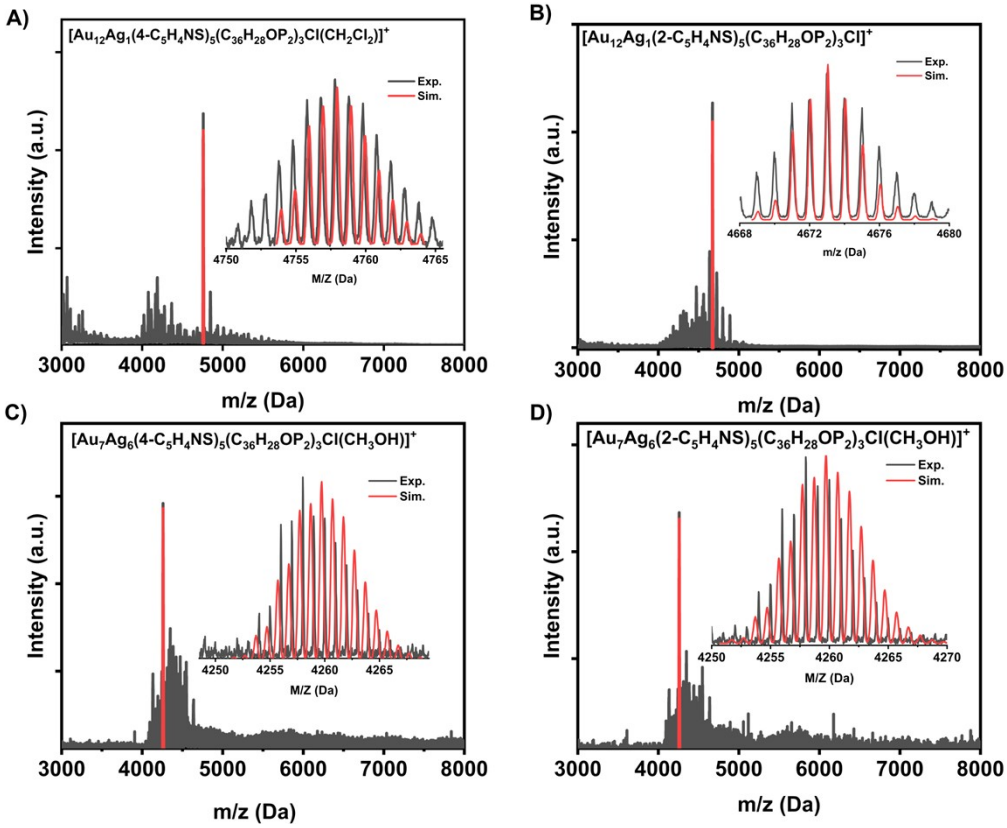

Figure S14. ESI-MS data of (A) **$Au_{12}Ag_1$-4-MPy**, (B) **$Au_{12}Ag_1$-2-MPy**, (C) **Au_7Ag_6-4-MPy** and (D) **Au_7Ag_6-2-MPy**.

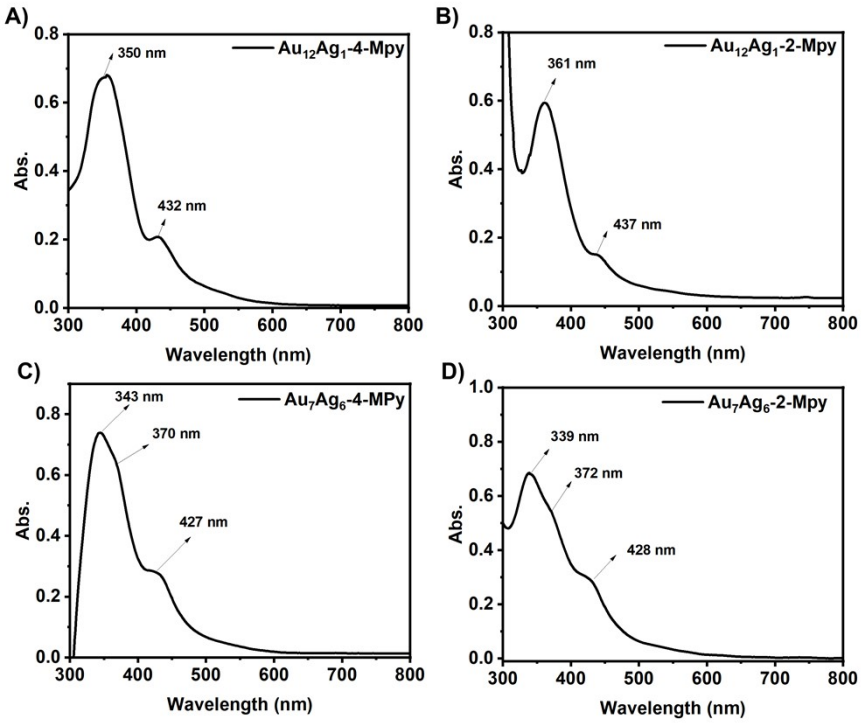

Figure S15. UV-vis spectra of (A) **$Au_{12}Ag_1$-4-MPy**, (B) **$Au_{12}Ag_1$-2-MPy**, (C) **Au_7Ag_6-4-MPy** and (D) **Au_7Ag_6-2-MPy** in DMSO solution.

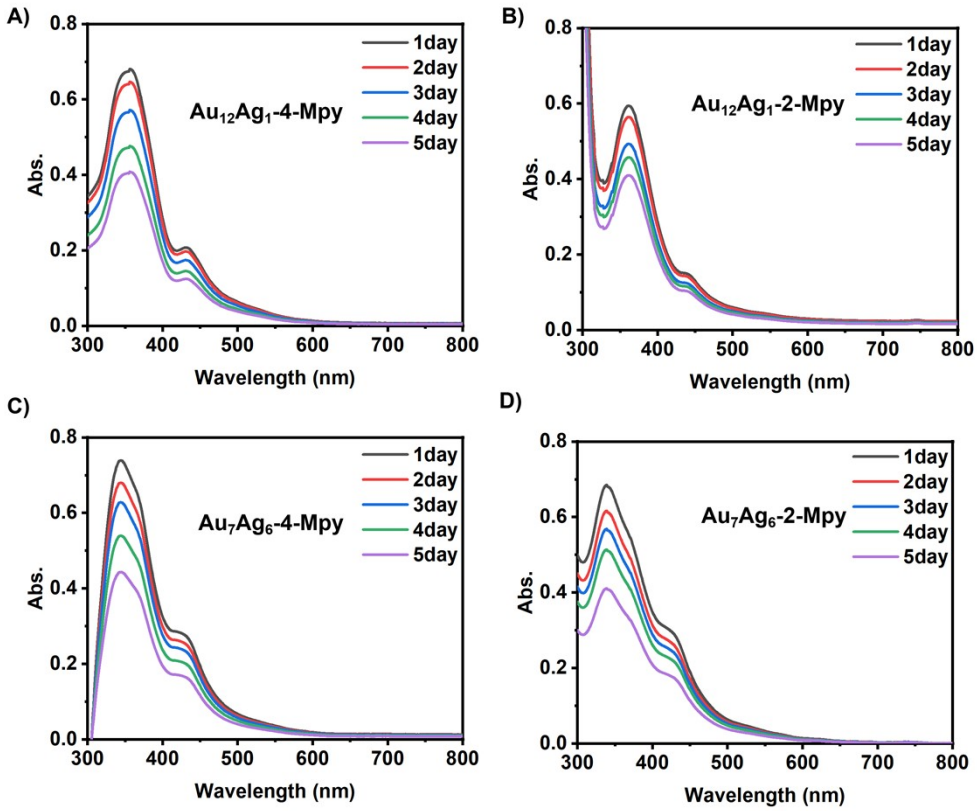

Figure S16. The UV-vis absorption spectra variation of (A) **$Au_{12}Ag_1$-4-MPy**, (B) **$Au_{12}Ag_1$-2-MPy**, (C) **Au_7Ag_6-4-MPy** and (D) **Au_7Ag_6-2-MPy** in DMSO solution. These nanoclusters show good stability in the ambient over 5 days.

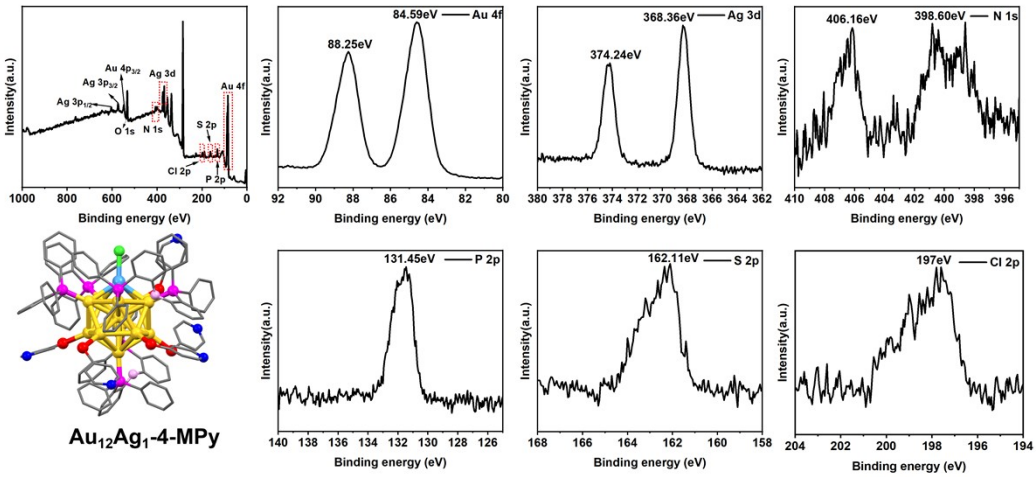

Figure S17. The XPS spectrum of **$Au_{12}Ag_1$-4-MPy** nanocluster.

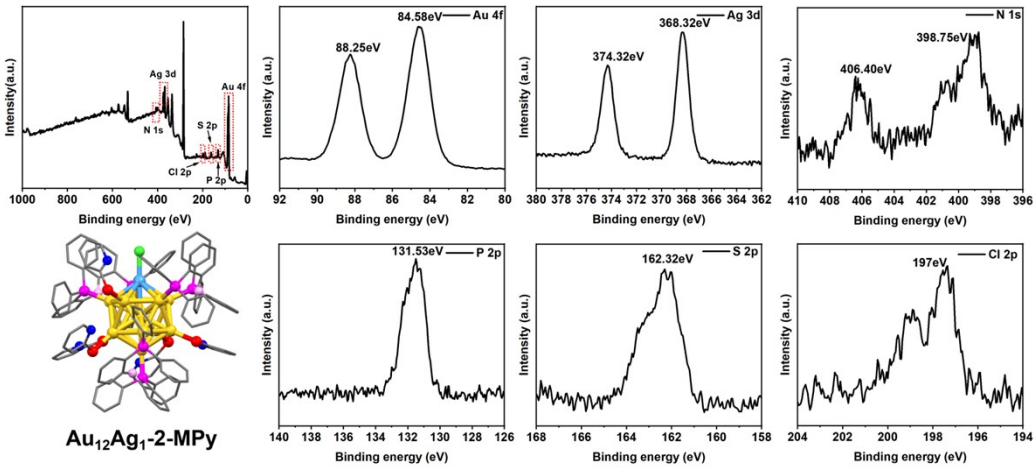

Figure S18. The XPS spectrum of **$Au_{12}Ag_1$-2-MPy** nanocluster.

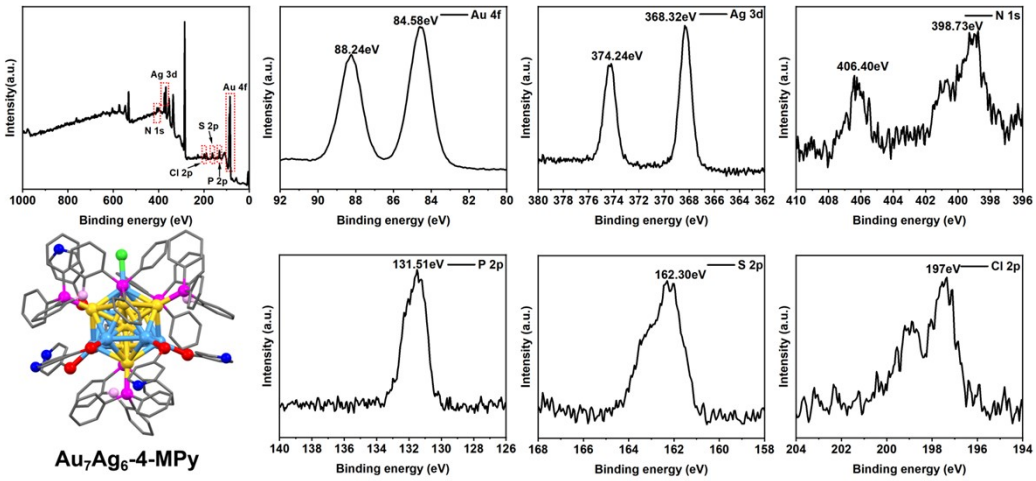

Figure S19. The XPS spectrum of **Au_7Ag_6-4-MPy** nanocluster.

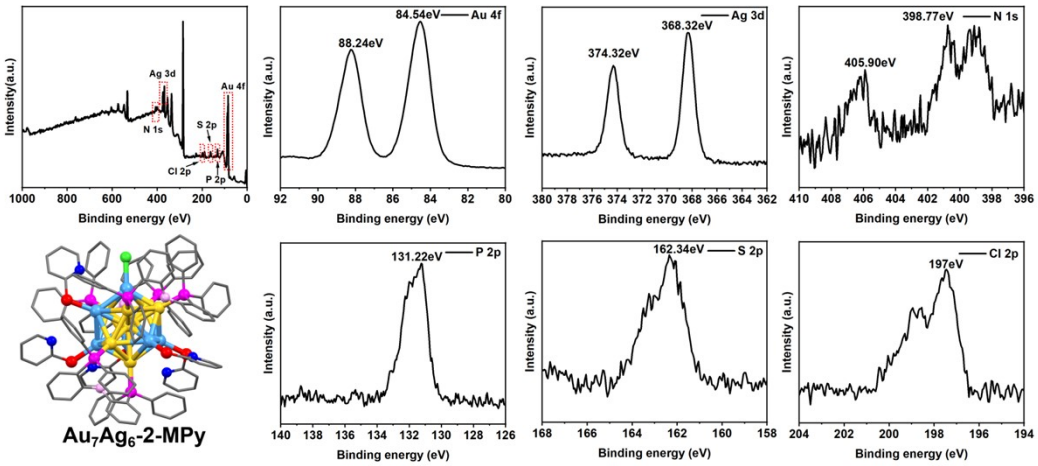

Figure S20. The XPS spectrum of **Au_7Ag_6-2-MPy** nanocluster.

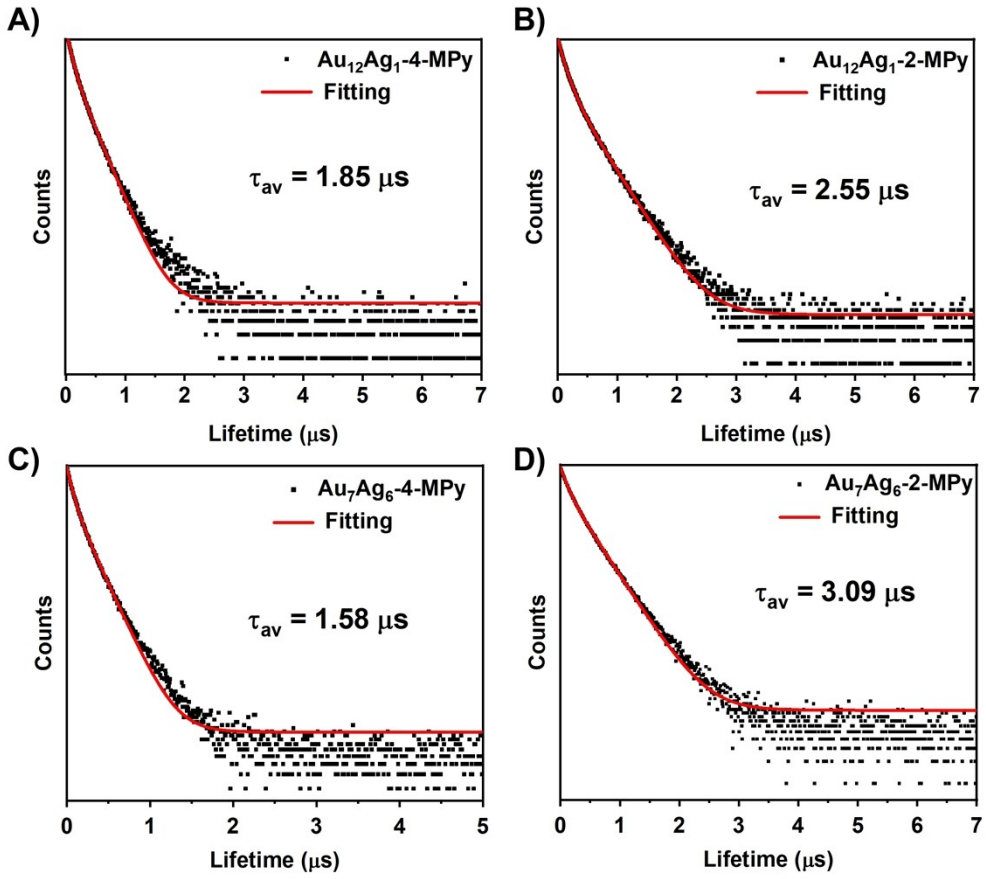

Figure S21. PL decay curves and fitting curves of (A) **$Au_{12}Ag_1$-4-MPy** and (B)**$Au_{12}Ag_1$-2-MPy** and (C) **Au_7Ag_6-4-MPy** and (D) **Au_7Ag_6-2-MPy**.

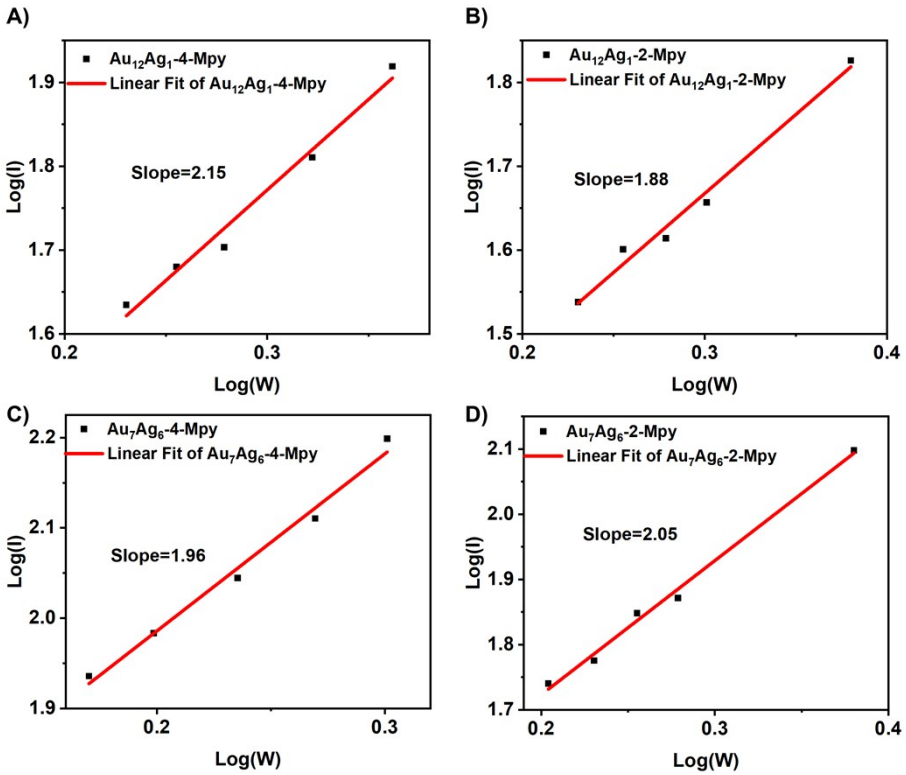

Figure S22. Two-photon fluorescence verification of (A) **$Au_{12}Ag_1$-4-MPy** and (B)**$Au_{12}Ag_1$-2-MPy** and (C) **Au_7Ag_6-4-MPy** and (D) **Au_7Ag_6-2-MPy**. (nanocluster concentration: 1 x 10^{-3} mol/L; excitation wavelength: 820 nm).

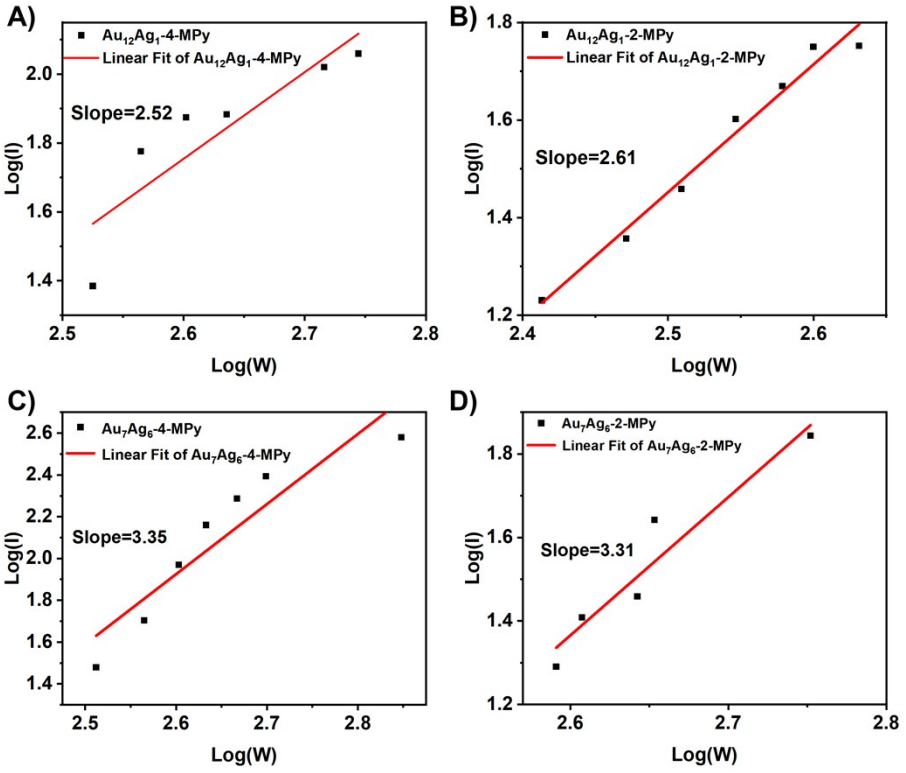

Figure S23. Three-photon fluorescence verification of (A) $Au_{12}Ag_1$-4-MPy and (B)$Au_{12}Ag_1$-2-MPy and (C) Au_7Ag_6-4-MPy and (D) Au_7Ag_6-2-MPy. ((nanocluster

concentration: 1 x 10^{-3} mol/L; excitation wavelength: 1200 nm).

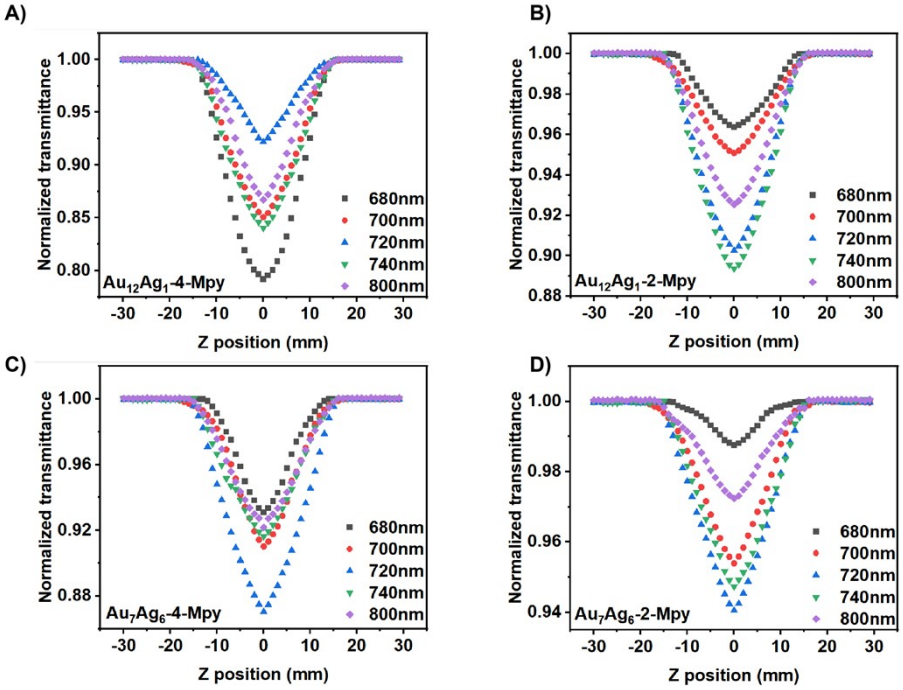

Figure S24. Two-photon absorption spectra of (A) $Au_{12}Ag_1$-4-Mpy, (B) $Au_{12}Ag_1$-2-Mpy, (C) Au_7Ag_6-4-Mpy, and (D) Au_7Ag_6-2-Mpy under excitation at 680-800 nm (nanocluster concentration: 1 x 10^{-3} mol/L) .

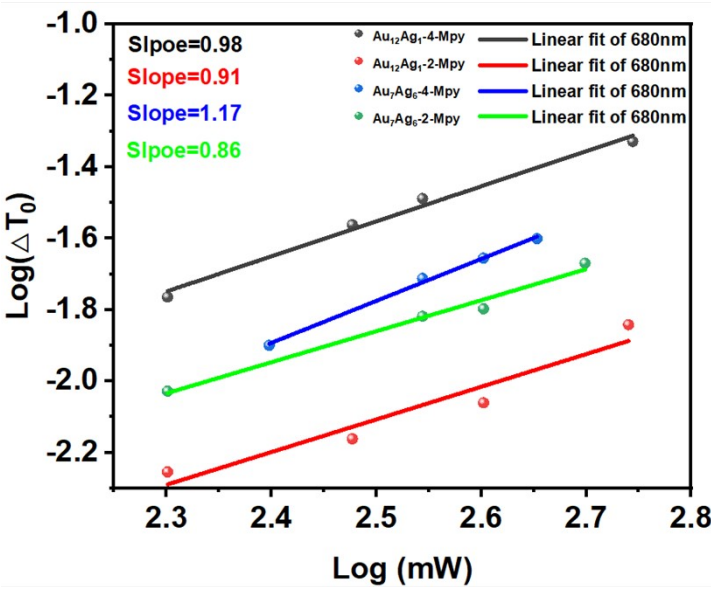

Figure S25. (A) Two photon absorption verification of $Au_{12}Ag_1$-4-Mpy, (B) $Au_{12}Ag_1$-2-Mpy, (C) Au_7Ag_6-4-Mpy, (D) Au_7Ag_6-2-Mpy under 680 nm excitation (nanocluster concentration: 1 x 10^{-3} mol/L).

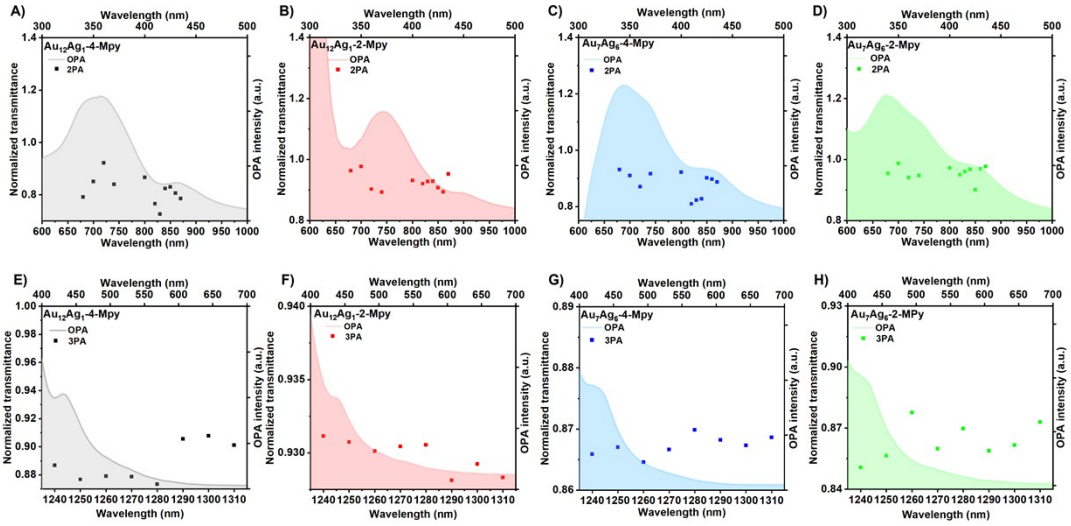

Figure S26. The correlation between wavelength-dependent two-photon absorption (left, lower axes) and single-photon absorption (OPA) spectra at twice the wavelength (right, upper axes) for (A) $Au_{12}Ag_1$-4-Mpy, (B) $Au_{12}Ag_1$-2-Mpy, (C) Au_7Ag_6-4-Mpy, (D) Au_7Ag_6-2-Mpy. The correlation between wavelength-dependent three-photon absorption (left, lower axes) and single-photon absorption (OPA) spectra at three times the wavelength (right, upper axes) for (E) $Au_{12}Ag_1$-4-Mpy, (F) $Au_{12}Ag_1$-2-Mpy, (G) Au_7Ag_6-4-Mpy, (H) Au_7Ag_6-2-Mpy.

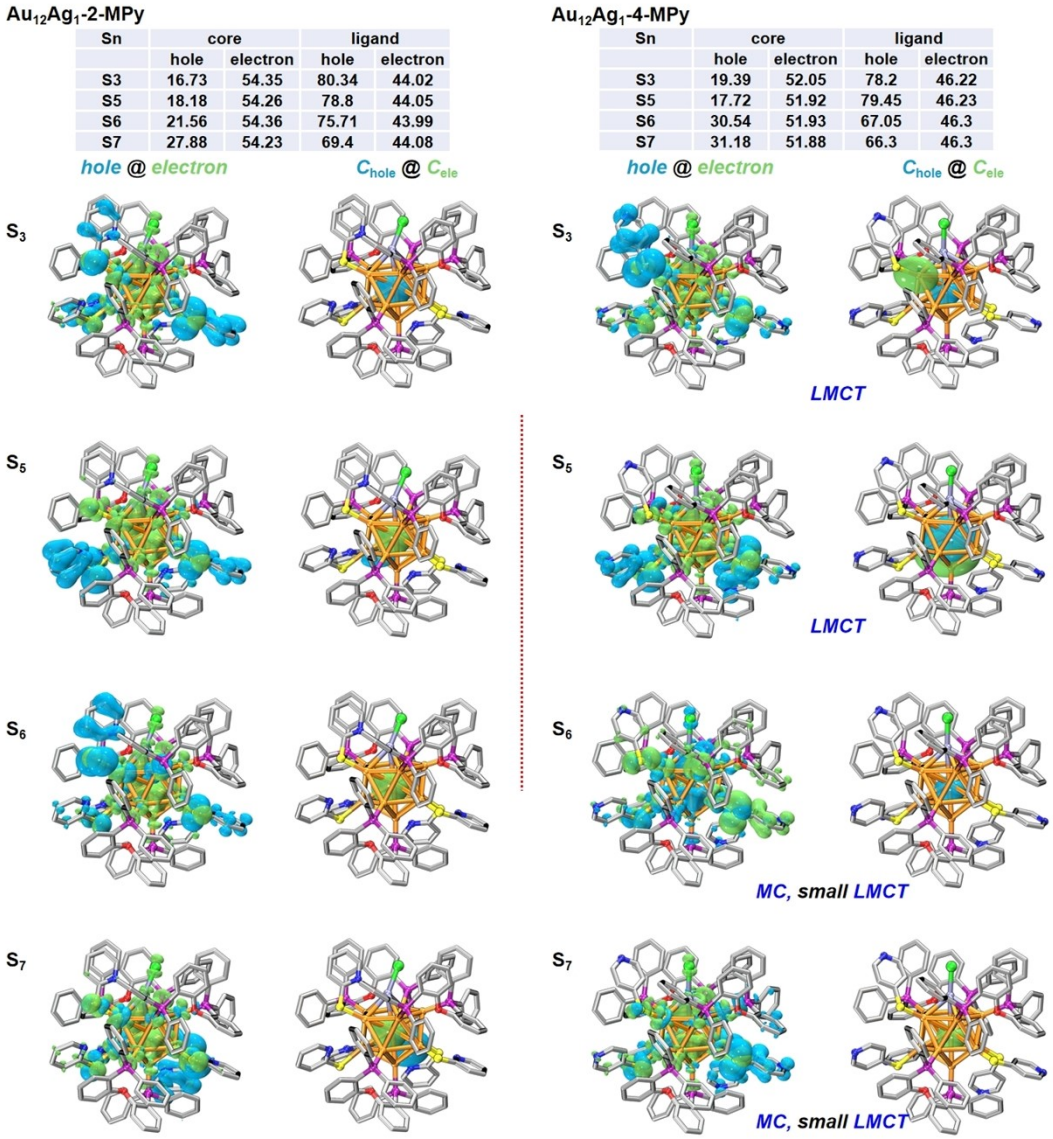

Figure S27. Hole and electron distributions of the S_3-S_7 state of $Au_{12}Ag_1$.

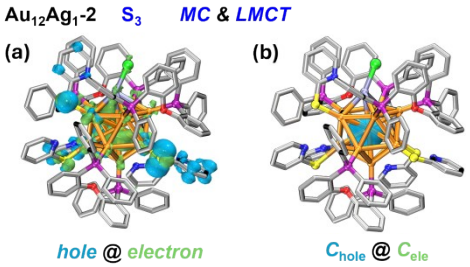

Figure S28. (a) Hole and electron distributions of the S_3 state of $Au_{12}Ag_1$-2-MPy including real-space distribution; (b) Smoothing of hole and electron isosurfaces.

Table S1. The quantum yield of nanoclusters.

NC	Liquid (%)	Solid (%)
$Au_{12}Ag_1$-4-Mpy	1.76	11.86
$Au_{12}Ag_1$-2-Mpy	2.28	23.77
Au_7Ag_6-4-Mpy	2.21	9.83
Au_7Ag_6-2-Mpy	3.07	12.23

Table S2. Radiative and non-radiative parameters obtained from PL measurements (QY: quantum yield, τ_{avg}: average lifetime, k_r: radiative decay rate, k_{nr}: non-radiative decay rate).

NC	QY (%)	τ_{avg}(μs)	$K_r(S^{-1})$	$K_{nr}(S^{-1})$
$Au_{12}Ag_1$-4-Mpy	1.76	1.85	9.5×10^3	5.31×10^5
$Au_{12}Ag_1$-2-Mpy	2.28	2.55	8.9×10^3	3.83×10^5
Au_7Ag_6-4-Mpy	2.21	1.58	14×10^3	6.2×10^5
Au_7Ag_6-2-Mpy	3.07	3.09	10×10^3	2.7×10^4

Table S3. Crystal data and structure refinement for $Au_{12}Ag_1$-2-MPy-OK.

Identification code	$Au_{12}Ag_1$-2-MPy-OK
Empirical formula	$C_{133}H_{104}AgAu_{12}ClN_5O_3P_6S_5$
Formula weight	4673.24
Temperature/K	120(2)
Crystal system	monoclinic
Space group	$P2_1/n$
a/Å	17.195(2)
b/Å	24.605(3)
c/Å	34.833(4)
α/°	90
β/°	93.887(9)
γ/°	90
Volume/Å^3	14703(3)
Z	4
Radiation	CuKα (λ = 1.54186)
2θ range for data collection/°	10.312 to 140.576
Index ranges	$-19 \leq h \leq 20$, $-11 \leq k \leq 29$, $-42 \leq l \leq 40$
Reflections collected	110168
Independent reflections	27158 [R_{int} = 0.0707, R_{sigma} = 0.0667]
Data/restraints/parameters	27158/1160/1231
Goodness-of-fit on F^2	1.039
Final R indexes [I>=2σ (I)]	R_1 = 0.0947, wR_2 = 0.2558
Final R indexes [all data]	R_1 = 0.1113, wR_2 = 0.2714
Largest diff. peak/hole / e Å^{-3}	4.17/-5.95

Table S4. Crystal data and structure refinement for $Au_{12}Ag_1$-4-MPy-OK.

Identification code	$Au_{12}Ag_1$-4-MPy-OK
Empirical formula	$C_{133}H_{104}AgAu_{12}ClN_5O_3P_6S_5$
Formula weight	4673.24
Temperature/K	120(2)
Crystal system	triclinic
Space group	P-1
a/Å	15.999(3)
b/Å	16.750(2)
c/Å	30.139(4)
α/°	86.732(12)
β/°	89.337(14)
γ/°	87.829(13)
Volume/Å^3	8057(2)
Z	4
Radiation	CuKα (λ = 1.54186)
2θ range for data collection/°	8.128 to 124.996
Index ranges	$-18 \leq h \leq 18$, $-14 \leq k \leq 19$, $-34 \leq l \leq 34$
Reflections collected	56629
Independent reflections	24737 [R_{int} = 0.0419, R_{sigma} = 0.0479]
Data/restraints/parameters	24737/1336/1291
Goodness-of-fit on F^2	1.066
Final R indexes [I>=2σ (I)]	R_1 = 0.0669, wR_2 = 0.1935
Final R indexes [all data]	R_1 = 0.0768, wR_2 = 0.2014
Largest diff. peak/hole / e Å^{-3}	3.41/-4.77

Table S5. Crystal data and structure refinement for Au_7Ag_6-2-MPy-OK.

Identification code	Au7Ag6-2-MPy-OK
Empirical formula	$C_{133}H_{104}Ag_6Au_7Cl_{0.97}N_5O_3P_6S_5$
Formula weight	4226.70
Temperature/K	120(2)
Crystal system	triclinic
Space group	P-1
a/Å	15.149(3)
b/Å	16.597(3)
c/Å	29.570(6)
α/°	86.556(16)
β/°	86.473(16)
γ/°	88.139(16)
Volume/Å^3	7404(3)
Z	2
Radiation	CuKα (λ = 1.54186)
2θ range for data collection/°	8.034 to 124.998
Index ranges	$-16 \leq h \leq 17$, $-15 \leq k \leq 19$, $-22 \leq l \leq 34$
Reflections collected	41333
Independent reflections	22446 [R_{int} = 0.0906, R_{sigma} = 0.0726]
Data/restraints/parameters	22446/1813/1292
Goodness-of-fit on F^2	1.083
Final R indexes [I>=2σ (I)]	R_1 = 0.1051, wR_2 = 0.2776
Final R indexes [all data]	R_1 = 0.1249, wR_2 = 0.2945
Largest diff. peak/hole / e Å^{-3}	3.64/-3.53

Table S6. Crystal data and structure refinement for Au_7Ag_6-4-MPy-OK.

Identification code	Au_7Ag_6-4-MPy-OK
Empirical formula	$C_{133}H_{104}Ag_6Au_{6.39}ClN_5O_3P_6S_5$
Formula weight	4107.61
Temperature/K	120(2)
Crystal system	triclinic
Space group	P-1
a/Å	15.832(3)
b/Å	16.707(3)
c/Å	29.996(5)
α/°	86.323(15)
β/°	88.797(14)
γ/°	87.481(15)
Volume/Å^3	7909(2)
Z	2
Radiation	CuKα (λ = 1.54186)
2θ range for data collection/°	6.234 to 129.998
Index ranges	$-13 \leq h \leq 18$, $-19 \leq k \leq 19$, $-35 \leq l \leq 27$
Reflections collected	65619
Independent reflections	26304 [R_{int} = 0.1161, R_{sigma} = 0.1076]
Data/restraints/parameters	26304/1209/1280
Goodness-of-fit on F^2	1.483
Final R indexes [I>=2σ (I)]	R_1 = 0.1469, wR_2 = 0.3603
Final R indexes [all data]	R_1 = 0.1731, wR_2 = 0.3795
Largest diff. peak/hole / e Å^{-3}	7.37/-8.38

Table S7. Two Photon Absorption Cross Sections of $Au_{12}Ag_1$-4-Mpy, $Au_{12}Ag_1$-2-Mpy, Au_7Ag_6-4-Mpy, and Au_7Ag_6-2-Mpy.

σ_2(GM) / **λ (nm)**	$Au_{12}Ag_1$-4-Mpy	$Au_{12}Ag_1$-2-Mpy	Au_7Ag_6-4-Mpy	Au_7Ag_6-2-Mpy
680	3688.62	1339.56	2522.5	805.26
700	2584.17	388.78	1636.03	402.53
720	916.76	1178.04	1017.61	718.74
740	1578.74	1073.06	867.45	536.98
800	1439.78	569.31	666.25	550.75
820	6290.93	1931.91	4468.79	1207.44
830	5755.49	1797.3	4334.19	994.08
840	4400.46	1728.75	4234.31	809.37
850	4609.87	1824.9	2368.49	1109.51
860	5142.4	2193.66	2609.58	775.2
870	5576.45	1100.11	2921	606.96

The maximum two-photon absorption cross-section of $Au_{12}Ag_1$-4-Mpy at 820 nm is 6290.93 GM;

The maximum two-photon absorption cross-section of $Au_{12}Ag_1$-2-Mpy at 860 nm is 2193.66 GM;

The maximum two-photon absorption cross-section of Au_7Ag_6-4-Mpy at 820 nm is 4468.79 GM;

The maximum two-photon absorption cross-section of Au_7Ag_6-2-Mpy at 820 nm is 1207.44 GM;

Table S8. Three Photon Absorption Cross Sections of $Au_{12}Ag_1$-4-Mpy, $Au_{12}Ag_1$-2-Mpy, Au_7Ag_6-4-Mpy, and Au_7Ag_6-2-Mpy.

σ_3 (10^{-73} cm^{6}s^{2}photon^{-2}) / **λ (nm)**	$Au_{12}Ag_1$-4-Mpy	$Au_{12}Ag_1$-2-Mpy	Au_7Ag_6-4-Mpy	Au_7Ag_6-2-Mpy
1240	0.965	1.754	1.692	1.600
1250	0.967	1.726	1.664	1.512
1260	0.970	1.714	1.645	1.417
1270	0.962	1.711	1.634	1.592
1280	0.946	1.682	1.628	1.523
1290	0.885	1.795	1.614	1.538
1300	0.864	1.018	1.609	1.529
1310	0.898	2.031	1.608	1.541

The maximum three-photon absorption cross-section of $Au_{12}Ag_1$-4-Mpy at 1260 nm is 0.97×10^{-73} cm6s^{2}photon^{-2};

The maximum three -photon absorption cross-section of $Au_{12}Ag_1$-2-Mpy at 1310 nm is 2×10^{-73} cm6s^{2}photon^{-2};

The maximum three -photon absorption cross-section of Au_7Ag_6-4-Mpy at 1240 nm is 1.69×10^{-73} cm6s^{2}photon^{-2};

The maximum three -photon absorption cross-section of Au_7Ag_6-2-Mpy at 1240 nm is 1.6×10^{-73} cm6s^{2}photon^{-2};